Singularity analysis by Pade approximants of some holomorphic maps



1994 J. Phys. A: Math. Gen. 27 6215

(http://iopscience.iop.org/0305-4470/27/18/029)

J. Phys. A: Math. Gen. 27 (1994) 6215–6229. Printed in the UK

# Singularity analysis by Padé approximants of some holomorphic maps

L Billi†, E Todesco‡ and G Turchetti‡

† SISSA, Via Beirut 4, Miramare 34013 Trieste, INFN, Sezione di Bologna, Italy

‡ Dipartimento di Fisica della Università, Via Irnerio 46, Bologna, INFN, Sezione di Bologna, Italy

Received 5 April 1994

**Abstract.** The analysis of the singularity structure of some series arising in the conjugation theory of holomorphic maps is performed using the Padé approximants. The validity of PA is checked for functions whose analytic structure is known: one observes that the numerical results are extremely sensitive to errors due to the use of a finite precision; normal or double precision used in FORTRAN codes is, in most cases, not sufficient to perform a numerical analysis of the singularity structure. In order to have significant results at high orders all the computations were carried out using codes which allow us to operate with a sufficiently large number of digits. The case of linearizable diffeomorphisms and of mappings tangent to the identity of $(\mathbb{C}, 0)$ was considered: PA of both the direct and the inverse conjugating functions of a quadratic map to its normal form were computed and a comparison was performed with analytical results when available. When the singularity pattern was unknown, the poles and the zeros of the PA provided a coherent picture, which in some cases allowed rigorous results to be established.

## 1. Introduction

The roots of integrability in dynamical systems are not yet understood but one can characterize the changes occurring between integrable and non-integrable systems by determining the singularities of the functions which conjugate each other. Non-integrable systems have a richer variety of topological structures in phase space since they have less symmetries. For Hamiltonian systems it is well known that nonlinear resonances change the topology of orbits, determining the appearance of singularities and the asymptotic character of the corresponding normal forms [1].

Even in the case of the simplest models, such as area preserving maps, the singularity analysis is difficult; some results have been obtained by combining perturbative and KAM estimates [2] and also by using low-order Padé approximants (PA) on the Fourier components [3]. The PA, which have been first applied to scattering problems in field theory and quantum mechanics [4–7], have also been used to detect the natural boundaries in the conjugation of a KAM curve with a circle for area preserving maps [8, 9].

In this paper we critically examine the use of Padé approximants [10] in the simpler case of the conjugation of mappings of the complex plane [11]. This problem is relevant for Hamiltonian dynamics: indeed the angle analyticity of an invariant curve of a standard map is closely related to the analyticity in the Siegel problem [12].

When the singularities of the conjugation function are known we can test the reliability of Padé approximants, and use them subsequently to explore the complex plane when no analyticity results are available. These tests are quite relevant because the construction of

0305-4470/94/186215+15$19.50  

rational approximations is very sensitive to the accuracy of the coefficients of the given series and high-order approximants computed with low accuracy typically have an abundance of poles accumulating on a closed curve (a circle), which is the natural boundary of a noise function [13] as first observed in a numerical experiment by Froissart [14]. To this end all the algorithms have been developed in arbitrary floating point precision, and up to several hundreds of decimal digits were used in the actual computations [15]. In order to separate the real singularities from noise singularities the residue analysis is crucial: the noise singularities have a residue which is proportional to the round-off accuracy, while the true singularities must have a bigger one. The analysis of residues allows one also to determine the quasi-analytic character of the function and the possibility of continuation across the natural boundaries [16, 17].

We first consider very elementary examples such as rational functions with poles on the real axis or on a circle, to illustrate how the number of significant digits affects the presence of noise singularities and how ordinary machine precision does not allow one to overcome low orders.

Following the investigation carried out by Xie [18] we examine the conjugation functions of a complex quadratic map $z' = \lambda z + z^2$ with its linear part $\zeta' = \lambda\zeta$, namely $\zeta = \Psi(z)$ and $z = \Phi(\zeta)$, when the Julia set [19] is connected.

If $0 < \lambda < 1$, $\Psi$ is analytic with a natural boundary on the Julia set and only very high-order Padé approximants ($N > 100$) reproduce such a pattern. The analytic structure of the conjugating function $\Phi$ was not known and the PA have allowed us to determine it: all the singularities are on the real axes starting at the image of the critical point of the map, and the residues all have the same sign. It can be proved that $\Phi$ is analytic in the cut plane and is a Stjeltjes function; the sheets of the Riemann surface are mapped into domains of the $z$-plane, which tasselate the Fatou set. If $1 < \lambda < 3$, then the poles of $\Psi$ are on the real negative axis and it can be proved that it is a Stjeltjes function. In both cases, the Stjeltjes property ensures uniform convergence of the PA to the function.

If $\lambda$ is complex with a resonant phase $2\pi p/q$, then the singularities are distributed on $q$ rays; if $\lambda = e^{i\omega}$, with $\omega/2\pi$ diophantine, they are all on a circle, whose image is the Siegel disc.

The resonant parabolic map $\lambda = e^{i2\pi p/q}$ is no longer linearizable [20]: in this case one conjugates a generic map to the normal form, called the resonant standard shift, which has explicit iteration and invariants. Using the Borel transform [21] or other techniques [22] one can prove that the conjugating function can be re-summed to $2kq$ functions analytic on sectors, where $k \in \mathbb{Z}$. We considered small perturbations of the standard shift in the case tangent to the identity $k = q = 1$, limiting our analysis to order one in the small parameter (homologic equation) [23]: we show that the PA reproduce the analytic structure of the Borel transform of the conjugating function. In the case of the formal series which define the conjugation function $\Psi$, there is a strong numerical evidence that the PA re-sum the formal series to the values of the two functions analytic on sectors.

In all the cases analysed, the role of precision is of great importance; in order to carry out significant analysis one has to compute high orders using a correspondingly high accuracy. The inspection of residues allows the detection of the presence of poles due to round-off errors. If the computations are carried out using standard precision, then the number of significant poles (i.e. poles which are not due to round-off errors) does not increase with the order of PA, and is usually so low that no useful information can be obtained.

The conclusion of the present work is that the PA are adequate to describe the singularity pattern of a conjugation function, especially when the singularity set is not a fractal boundary.

The plan of the paper is the following. In section 2 we introduce the definition of Padé approximants and analyse the influence of the noise due to the machine round-off error for two functions having simple poles respectively on a straight line and on a circle. In section 3 the case of linearizable mappings of $(\mathbb{C}, 0)$ is considered: the analytic structure of both conjugation functions is analysed through the PA, and the relation with the Julia set and the precision needed to obtain significant results are discussed. The case of mappings tangent to the identity, which are not linearizable, is considered in section 4: the conjugation to the normal form (i.e. the standard shift) is analysed in the homologic case; the analytic structure of the inverse conjugating function $\Psi$ and its Borel transform is obtained with analytic tools and a comparison with the results of the PA is given.

## 2. Padé approximants and noise

Given an analytic function $f(z)$, $z \in \mathbb{C}$, with Taylor expansion $f(z) = f_0 + f_1 z + \cdots + f_n z^n + \cdots$ (convergent or asymptotic), its $[M/N]$ Padé approximants are defined by

$$[M/N]_f(z) \equiv \frac{P_M(z)}{Q_N(z)} = f(z) + \mathrm{O}\left(z^{N+M+1}\right) \tag{2.1}$$

where $P_M$ and $Q_N$ are polynomials in $z$ of maximum order $M$ and $N$, respectively. If $f(z)$ is a Stjeltjes function [10], the sequence $[N-1/N]$, whose partial fraction expansion reads

$$[N-1/N]_f(z) = \sum_{k=1}^{N} \frac{\gamma_k^{(N)}}{z - z_k^{(N)}} \qquad \gamma_k^{(N)}, z_k^{(N)} \in \mathbb{C} \tag{2.2}$$

converges uniformly for $N \to \infty$ to $f(x)$ in any compact not intersecting the singularity set $\mathcal{S}$, and the poles, which in the limit belong to $\mathcal{S}$, have positive residues. This property, due the orthogonality of the polynomials $z^N Q_N(1/z)$, does not extend to other classes of functions, for which weaker convergence results (in measure or capacity) hold [24, 25].

Letting $\mathcal{P}_N = \cup_{k=1}^{N} z_k^{(N)}$ one could expect that if for any $N$ one can find a subset $\hat{\mathcal{P}}_N \subset \mathcal{P}_N$ such that the sequence $\hat{\mathcal{P}}_N$ converges with respect to the Hausdorff distance, then the closure of the limit set is $\mathcal{S}$ (in this way we exclude the wandering poles which determine the weak convergence to the function).

In general, the distribution of zeros and poles provides some useful hint on the singularity structure of the function; however, their numerical computation is usually non-trivial. Indeed the accuracy achieved on the coefficients of $P_{N-1}$, $Q_N$ with any of the algorithms (linear equations, continued fraction, recurrent relations) is basically the same and depends critically on the number of significant digits used in the calculations. To obtain all the zeros and poles of the $[N-1/N]$ PA within a desired accuracy all the computations have to be carried out with a number $d$ of digits monotonically increasing with $N$. If $d$ is kept constant, while $N$ is increased, a natural boundary due to round-off errors appears. Indeed the effect of using $\epsilon = 10^{-d}$ accurate arithmetic is equivalent to replacing the function $f(z)$ with another function $f_\epsilon(z)$:

$$f_\epsilon(z) \equiv f(z) + \epsilon r(z) = \sum_{n=0}^{\infty} f_n(1 + \epsilon r_n) z^n \qquad \epsilon = 10^{-d} \tag{2.3}$$

where $r(z)$ is a function with random coefficients $r_n$ [26]. If $f_n = 1$ and $r_n$ are random variables uniformly distributed in a compact set such as $[-1, 1]$, then the convergence radius

is still 1; the poles of the PA of $f_\epsilon$ are with probability 1 on the unit circle, which is a natural boundary [13]. If $f_n \neq 1$, the convergence radius $R$ of $r(z)$ is the same as $f(z)$ and $r(z)$ has a natural boundary on the disc of radius $R$. The poles of the PA due to noise have a residue proportional to $\epsilon$; this phenomenon was first observed by Froissart [14], who studied the noise effect on the function $f(z) = (1-z)^{-1}$ discovering that beyond the stable pole at $z = 1$ the remaining poles are distributed on the unit circle; each pole due to the noise has a nearby zero of the function $f$ at distance $\epsilon$, and the residue of the pole is also of order $\epsilon$. In some numerical examples it is observed that a few poles of $[N-1/N]$ and $[N/N]$ PA due to the noise are located at the interior of the convergence disk. Even though one could expect that the internal poles migrate to the boundary of the disc $\gamma$ as $N \to \infty$, it is worthwhile remarking that the observed property is true (Szego theorem [27]) for the polynomials orthogonal with respect to a positive (random) measure on $\gamma$ which differ from the denominator of the Padé approximants†.

In this section we analyse two examples: a rational fraction with poles on the real axis, and a rational fraction with poles on the unit circle. Let

$$f(z) = \sum_{k=1}^{N} \frac{k^{-1}}{k-z} \tag{2.4}$$

be a rational fraction for which $[n-1/n]_f(z) = f(z)$ for $n \geqslant N$. We observe that

$$f_n = \sum_{k=1}^{N} \frac{1}{k^{n+2}} \tag{2.5}$$

so that the last coefficient $f_{2N-1}$ needed to compute the $[N-1/N]$ Padé is given by

$$f_{2N-1} = 1 + \sum_{k=2}^{N-1} \frac{1}{k^{2N+1}} + \frac{1}{N^{2N+1}} \tag{2.6}$$

and the last term is the contribution of the last pole to the coefficient $f_{2N-1}$. We expect that, using a precision of $d$ digits, the $N$th pole can be reproduced with an accuracy of $d_0$ digits if its contribution $N^{-2N-1}$ to the coefficient $f_{2N-1}$ is at least of order $10^{-(d-d_0)}$; this leads to the estimate

$$d = d_0 + (2N+1)\log_{10} N\,. \tag{2.7}$$

For $N = 10$ and $d_0 = 8$ we have $d = 29$ corresponding to ordinary quadruple precision, while for $N = 100$ we have $d = 410$. In figure 1 we show the results for $N = 50$ by displaying the poles of the [49/50] PA for $d = 20$ and $d = 200$‡. In the first case the noise disc is very evident and their residues are $\sim 10^{-20}$, in the second case the true poles are well reproduced and no noise effect is present. The second function we consider is given by

$$f_m(z) = \sum_k \frac{1}{1 - z e^{i2\pi k\omega}} \qquad k\omega \bmod 1 \in \mathcal{D}_m \tag{2.8}$$

† The orthogonal polynomials $\hat{Q}_N$ with respect to a positive measure and the denominators $Q_N$ of the $[N-1/N]$ PA are related by $\hat{Q}_N(x) = x^N Q_N(1/x)$ only if the support of the measure is on the real axis.

‡ Throughout the paper the zeroes of $Q_N(z)$ (even when the construction of the PA was carried out at low accuracy) were computed with high accuracy ($d = 200$), using a routine based on the Laguerre method: the zeroes were checked by evaluating the polynomial.

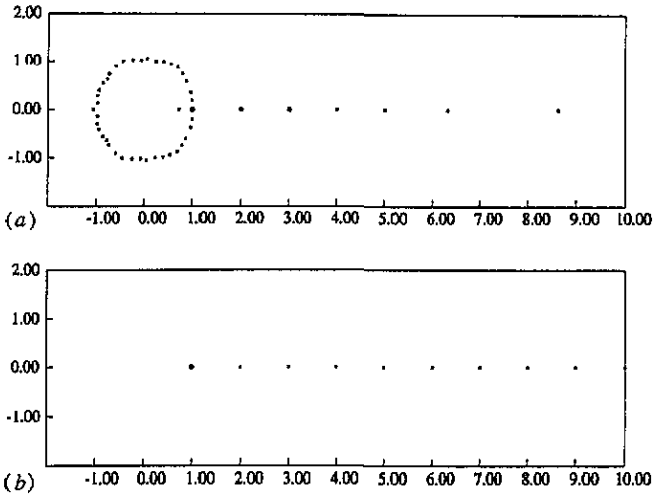


**Figure 1.** Poles of [49/50] PA of function 1 with (*a*) $d = 20$, (*b*) $d = 200$. The size of the dots is proportional to the logarithm of the absolute value of the residues.

where $\omega$ is the golden mean $(\sqrt{5} - 1)/2$ and $\mathcal{D}_m$ is a closed symmetric subset of $[0, 1[$ defined by the union of the intervals $[2k/(2m), (2k + 1)/(2m)]$ for $k = 0, \ldots, m - 1$ if $m \geqslant 1$, and $[0, 1[$ itself for $m = 0$. If $m = 0$, the poles distribution tends to be uniform on the circle as $N \to \infty$; the effect of noise is not relevant up to comparatively higher orders such as $N = 50$ for $d = 20$. For low values of $m$ the distribution is far from uniform and the effect of noise is more important; unless a careful examination of the residues is made it is difficult to distinguish the support of poles working at low accuracy. The same phenomenon would be observed if the poles are distributed on the partitions of a Cantor set.

## 3. Linearizable maps

We consider the linearization of a polynomial map

$$z' = F(z) = \lambda z + f(z) \qquad z \in \mathbb{C} \tag{3.1}$$

where $f(z)$ is a polynomial and $|\lambda| \neq 1$ or $\lambda = e^{i\omega}$ with $\omega/2\pi$ a Brjuno number [28]; it is well known that under such conditions $F(z)$ is analytically conjugated to its linear part. It follows that any two polynomial maps with the same linear part $\lambda z$ are analytically conjugated and therefore, without loss of generality, we shall restrict our analysis to the quadratic map. The multiplier $\lambda$ is the topological invariant of the map and determines the topology of the orbits.

We define the conjugating function $\Phi(\zeta)$ according to

$$z = \Phi(\zeta) = \zeta + \phi(\zeta) \qquad \phi(\zeta) = \sum_{n=2}^{\infty} \phi_n \zeta^n \tag{3.2}$$

so that the linearized map reads

$$\zeta' = \lambda \zeta \tag{3.3}$$

and $\Phi, \phi$ are implicitly defined by

$$F \circ \Phi(\zeta) = \Phi(\lambda\zeta) \qquad \phi(\lambda\zeta) - \lambda\phi(\zeta) = f(\zeta + \phi(\zeta)). \tag{3.4}$$

The inverse function $\Psi(z) \equiv \Phi^{-1}(z)$

$$\zeta = \Psi(z) = z + \psi(z) \qquad \psi(z) = \sum_{n=2}^{\infty} \psi_n z^n \tag{3.5}$$

satisfies the functional equation

$$\Psi \circ F(z) = \lambda\Psi(z) \qquad \psi(\lambda z + f(z)) - \lambda\psi(z) = -f(z). \tag{3.6}$$

In the quadratic case $f(z) = z^2$ the recurrences are very simple and letting $\phi_1 = \psi_1 = 1$ we have for $n \geqslant 2$

$$\phi_n = \frac{1}{\lambda^n - \lambda} \sum_{k=1}^{n-1} \phi_k \phi_{n-k} \qquad \psi_n = \frac{1}{\lambda - \lambda^n} \sum_{k=1}^{[n/2]} \binom{n-k}{k} \psi_{n-k} \lambda^{n-2k}. \tag{3.7}$$

A simple estimate based on majorant series gives a convergence radius for $\phi$ of at least $|\lambda|(1 - |\lambda|)/4$.

*3.1. Real multiplier:* $\lambda = e^{-\alpha} < 1$

We first consider the case of a quadratic map with $\lambda$ real. This map has two fixed points, an attractive one at the origin and a repulsive one at $z = 1 - \lambda$, while its critical point is at $z_c = -\lambda/2$. The function $\Psi(z)$ is analytic within the Fatou set $\mathcal{F}$ [19] and is given by

$$\Psi(z) = \lim_{n\to\infty} \frac{F^{\circ n}(z)}{\lambda^n} \qquad \forall z \in \mathcal{F}. \tag{3.8}$$

As a consequence we expect that for $0 < \lambda < 1$ the poles and zeros of the PA accumulate on the Julia set $\mathcal{J}$, which is connected in this parameter range. We also recall that $\mathcal{J}$ is the closure of the unstable fixed points of the map and that the preimages $F^{\circ -n}(z_c)$ of the critical point accumulate on $\mathcal{J}$ [19]. When $\lambda = \pm 1$ the map is no longer linearizable since $F$ or $F^{\circ 2}$ are tangent to the identity; for $\lambda = 1$ this is evident since the attractive and repulsive fixed points collapse.

In figures 2 and 3 we display the poles of the $[100/100]_\Psi(z)$ PA computed with different numbers $d$ of decimal digits, and compare them with the Julia set. The distribution of the poles and of the zeros follows the Julia set very closely, in the case of high accuracy computation (see figure 2), whereas it has a very poor resemblance when the accuracy is low (see figure 3). At the lowest accuracy the noise circle prevails and gradually the Julia set emerges from evident competition with noise. Even more interesting is the structure of the direct function $\Phi(\zeta) = \Psi^{-1}(\zeta)$. Also in this case with moderate accuracies the noise circle is still well present and only at the accuracy of $d = 200$ does it disappear—see figure 4. The emerging analytic structure is surprisingly simple, all the poles are on the real negative axis and their residues have the same sign, and it can be proved that $\Phi$ is a

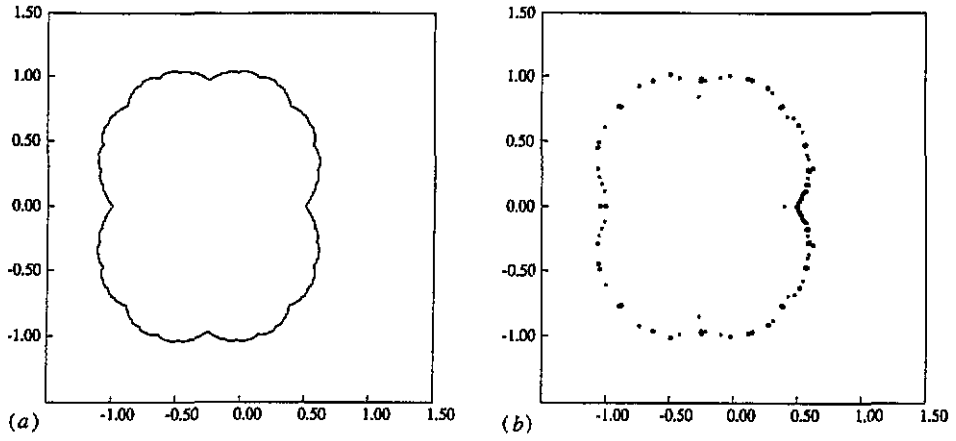


**Figure 2.** Julia set of the quadratic map with (*a*) $\lambda = \frac{1}{2}$ and (*b*) poles of $[100/100]_\Psi$ for $d = 200$.

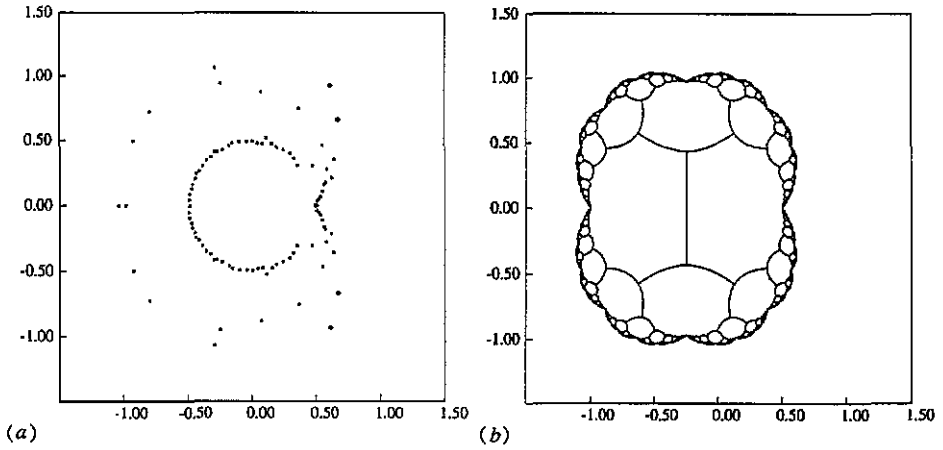


**Figure 3.** (*a*) Poles of $[100/100]_\Psi$ for the quadratic map with $\lambda = \frac{1}{2}$ computed with $d = 16$ and (*b*) tasselation of the analyticity domain of $\Psi$ into univalence domains.

Stjeltjes function. It can be checked that the first pole $\zeta_c$ is the image of the critical point $\zeta_c = \Psi(z_c)$.

The above-quoted properties can be explained according to the following scheme. Let us denote by $F_\pm^{-1}$ the inverse functions of $F$:

$$F_\pm^{-1} = \frac{-\lambda \pm \sqrt{\lambda^2 + 4z}}{2} \tag{3.9}$$

then the preimages of the critical point are

$$z_0 \equiv z_c \qquad z_k \equiv F_k^{-1}(z_c) \quad \dots \quad z_{k_1,\dots,k_n} \equiv F_{k_n}^{-1} \circ \dots \circ F_{k_1}^{-1}(z_c) \qquad k_i = \pm 1\,. \tag{3.10}$$

One can prove that $z_{k_1,\dots,k_n}$ are critical points of $\Psi$: in fact, differentiating (3.6), we have $\Psi'(F(z))\,F'(z) = \lambda\Psi'(z)$ and consequently for $z = z_c$, since $F'(z_c) = 0$, we have that

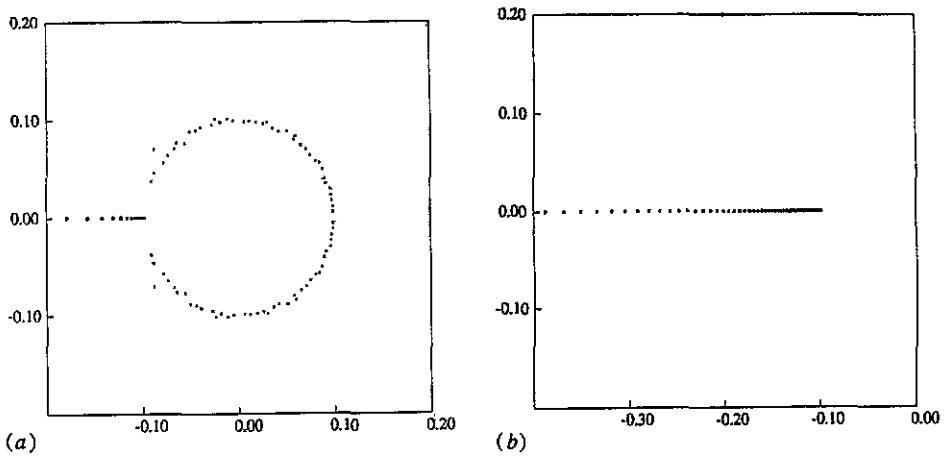


**Figure 4.** Poles of $[100/100]_\Phi$ for the quadratic map with $\lambda = \frac{1}{2}$ computed with (*a*) $d = 16$ and (*b*) $d = 200$.

$\Psi'(z_c) = 0$. A similar argument holds for the preimages of $z_c$. Moreover, one has that $\Psi(z_{k_1,\ldots,k_n}) = \lambda^{-n}\Psi(z_c)$: this can be proved by writing (3.6) as $\Psi(F^{-1}(z)) = \lambda^{-1}\Psi(z)$, which implies $\Psi(z_{k_1,\ldots,k_n}) = \lambda^{-n}\Psi(z_c)$. The images of the critical points of $F$ under the transformation $\Psi$ are the poles of $\Phi$, which are therefore $\zeta_c$, $\lambda^{-1}\zeta_c, \ldots, \lambda^{-n}\zeta_c$. This explains the pattern shown in figure 4. The tessellation of the analyticity domain of $\Psi$ in domains where $\Psi$ is injective is shown in figure 3(*b*). Each domain of the tasselation is mapped through $\Psi$ into a sheet of the Riemann surface of $\Phi$.

*3.2. Real multiplier:* $3 > \lambda = e^{\alpha} > 1$

In this case it is well known from Poincaré's theorem that $\Phi(\zeta)$ is an entire function. Indeed by majorant series one proves that $\Phi$ is analytic in a disc and the relation $\Phi(\zeta) = F^{\circ n} \circ \Phi(\lambda^{-n}\zeta)$ allows one to extend the analyticity to a disc of radius $\lambda^n r$ and, $n$ being arbitrary, $\Phi(\zeta)$ is entire. When $\lambda = 2$ in the quadratic case one has $\Phi(\zeta) = e^{\zeta} - 1$. For $\lambda > 1$, the origin becomes an unstable fixed point and the Julia set is no longer an obstruction to the conjugation with the linear expanding map; the obstruction appears at the stable fixed point.

The poles of the PA to $\Phi$ are located on a circle of large radius, as is usual for entire functions. The poles of high accuracy PA of $\Psi(z)$ are located on the half line $]-\infty, z_A]$, where $z_A = 1 - \lambda$ is the attractive fixed point and the residues are all positive, and it can be proved that $\Psi$ is a Stjeltjes function. The situation is analogous to the previous case, where now the roles of $\Psi$ and $\Phi$ are interchanged. The iterate of $z_c$ falls on the cut since $F(z_c) \leqslant z_A$ and it is now false that the critical point of $F$ and its preimages are critical points of $\Psi$ (we remark also that $\lambda^{-n}\zeta_c$ accumulate at the origin). Conversely, differentiating (3.4), one has

$$\lambda\Phi'(\lambda\zeta) = F'(\Phi(\zeta))\Phi'(\zeta) \tag{3.11}$$

and since $\zeta_c$ is a regular point of $\Phi(\zeta)$, and $F'(\Phi(\zeta_c)) \equiv F'(z_c) = 0$, it follows that $\Phi'(\lambda\zeta_c) = 0$. Similarly, differentiating (3.4) iterated $n$ times one proves that $\Phi'(\lambda^n\zeta_c) = 0$. Therefore, we have proved that the function $\Phi$ has critical points at $\lambda^n\zeta_c$ where $\Phi(\zeta_c) = z_c$ and on their images $\Phi(\lambda^n\zeta_c) = F^{\circ n}(z_c)$ the function $\Psi$ has square-root-type branch points. For $\lambda = 2$ we have a limit case since the image of the critical point is $\zeta_c = -\infty$ and the function $\Phi$ is injective in the whole complex plane.

### *3.3. Complex multiplier:* $\lambda = e^{-\alpha+i2\pi p/q}$

When the coefficient $\lambda$ in the map (3.1) is complex, $\lambda = \lambda_q \equiv \exp[i2\pi p/q - \alpha]$ with $\alpha$ real positive and $p, q$ two integer numbers with no common divisor, the analyticity properties of the conjugation function are similar to the case of $\lambda$ real. The main difference is that $\Phi(\zeta)$ is now analytic in the $\zeta$-plane cut along $q$ rays rather than a single one. Indeed in this case the pre-images of the critical points $z_{k_n,\ldots,k_1}$ are mapped into $\zeta_n = e^{n\alpha+i2\pi np/q}$ and these spiralling points are organized into $q$ half lines. This is confirmed by numerical computations: in figure 5(*a*) we show for $p = 1, q = 3$ the poles of the PA to the function $\Phi$ which at high accuracy are organized on three lines, whereas at low accuracy the competition with the noise circle makes them barely recognizable.

We have checked that the starting points of the rays are just the $\Psi$ transforms of the critical point and its $q - 1$ pre-images. The function in this case is analytic in the $\zeta$-plane cut along $q$ rays and on each ray there is a sequence of branch points of square-root type; each Riemann sheet is mapped into a domain where $\Psi$ is single-valued. This tasselation of the Fatou set can be explicitly constructed [29].

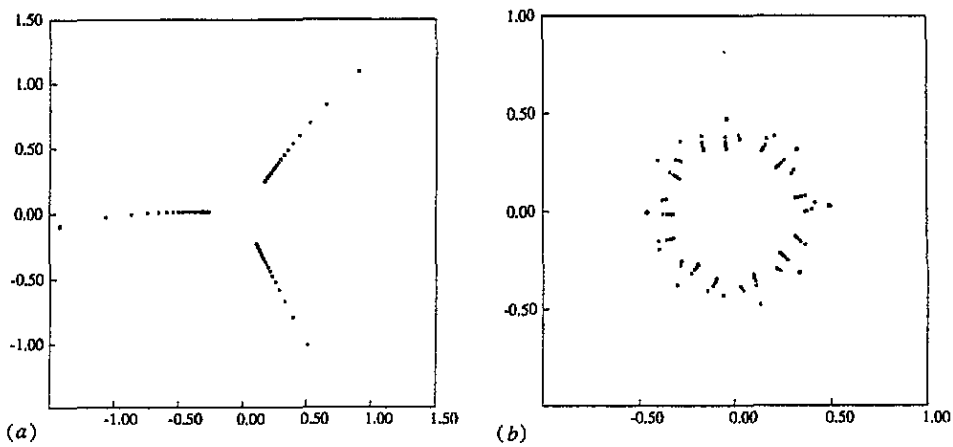


**Figure 5.** Poles of (*a*) $[100/100]_\Phi$ for the quadratic map with $\lambda = 0.9e^{2\pi i/3}$ computed with $d = 200$ and of (*b*) $[150/150]_\Phi$ with $\lambda = 0.99e^{2\pi i\omega}$, $d = 200$ and $\omega$ set to the golden mean.

### *3.4. The Siegel case:* $\lambda = e^{i\omega}$

We have analysed the case of $\lambda = e^{i\omega-\alpha}$ for $\omega/2\pi$ irrational and equal to the golden mean $(\sqrt{5} - 1)/2$ for $\alpha > 0$; the limit case $\alpha = 0$ corresponds to the Siegel problem. For $\alpha > 0$ the Padé show several rays which can still be interpreted as cuts emerging from the points $\zeta_n = e^{\alpha n+in\omega}$ which spiral to $\infty$. When $\alpha \to 0$ all the rays converge densely to a circumference of finite radius, whose image in the $z$-plane is the boundary of the Siegel disc, which is a fractal obtained by iterating the critical point. We consider the poles of the PA, computed with high accuracy, as $\alpha$ approaches zero and their distribution fully confirm the above picture, and show a hierarchical organization corresponding to the leading resonant approximations $p/q$ to the golden mean ($q = 13$ in figure 5(*b*)). When $\alpha = 0$ almost all the poles are on the boundary of the disc $|\zeta| = r_s$ and no pole is inside; in this case the effect of noise is not relevant, as observed for the function (2.8).

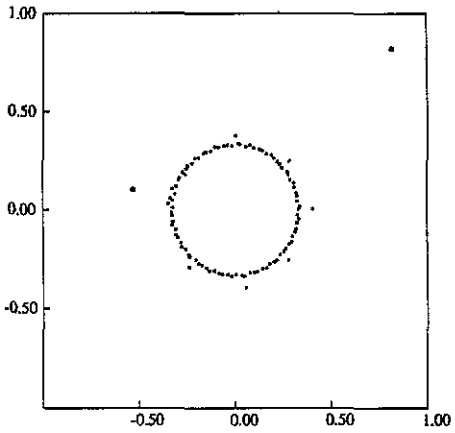


**Figure 6.** Poles of $[100/100]_\Phi$ PA for the Siegel problem with golden mean frequency with $d = 200$.

The Siegel problem is relevant since it is closely related to the circle map or the standard map if we let $z = e^{i\theta}$ and consider the analyticity properties in the complexified angle $\theta$, as proposed in [30, 31].

## 4. Non-linearizable maps

We consider a map tangent to the identity $\lambda = 1$; in this case a map having a non-zero quadratic term can be formally conjugated to

$$z' = z - z^2 + (1 - \gamma)z^3 \tag{4.1}$$

where $\gamma$ is a parameter which depends on the map we are considering, and is called the formal invariant [20–33]. The conjugation equation is more conveniently written by changing the variable according to $w = z^{-1}$ so that the map becomes $\overline{F}(w) = 1/F(w^{-1})$:

$$w' = \overline{F}(w) = w + 1 + \frac{\gamma}{w} + \overline{f}(w) \qquad \overline{f}(w) = O(w^{-2}). \tag{4.2}$$

The normal form in the case tangent to the identity is the standard shift [20, 34]

$$\zeta' = \frac{\zeta}{1 + \zeta} \tag{4.3}$$

which in the inverse coordinates $\eta = \zeta^{-1}$ takes the form $\eta' = \eta + 1$. The standard shift is an integrable map and has explicit iteration and interpolating flow: the orbits in normal coordinates are interpolated by the straight lines $\eta(t) = \eta_0 + t$ parallel to the real axis and their images in the $\zeta$-plane, $\zeta(t) = \zeta_0(1 + t\zeta_0)^{-1}$ are families of circles tangent to the real axis at the origin.

The conjugation function $\overline{\Psi}(w) = 1/\Psi(z)$ satisfies the functional equation $\overline{\Psi} \circ \overline{F} = \overline{\Psi} + 1$; choosing $\overline{\Psi}(w) = w - \gamma \log w + \overline{\psi}(w)$, where $\overline{\psi} = O(w^{-1})$, one has

$$\overline{\psi}\left(\overline{F}(w)\right) - \overline{\psi}(w) = \gamma\left(\log\frac{\overline{F}(w)}{w} - \frac{1}{w}\right) - \overline{f}(w). \tag{4.4}$$

The RHS of (4.4) is $O(w^{-2})$ and the formal solution $\overline{\psi}(w)$ is therefore well defined.

We analyse mappings which are small perturbations of the standard shift

$$w' = w + 1 + \epsilon \overline{f}(w) \qquad \text{or} \qquad z' = F(z) = \frac{z}{1+z} - \epsilon \frac{z^2}{(1+z)^2} f(z) + O(\epsilon^2) \tag{4.5}$$

where $\overline{f}(w) = O(w^{-2})$ so that the formal invariant is preserved. We consider the homologic equation [23], i.e. conjugation at the first order in $\epsilon$, which is assumed to be a small parameter; letting $\Psi(z) = z + \epsilon\psi(z) + O(\epsilon^2)$ and $\overline{\Psi}(w) \equiv 1/\Psi(w^{-1}) = w + \epsilon\overline{\psi}(w) + O(\epsilon^2)$ where $w = z^{-1}$, the equations satisfied by $\psi$ and $\overline{\psi}$ read

$$\overline{\psi}(w+1) - \overline{\psi}(w) = -\overline{f}(w) \qquad \psi\left(\frac{z}{1+z}\right) - \psi(z) = -f(z)\,. \tag{4.6}$$

We have two solutions $\overline{\psi}_1(w)$, $\overline{\psi}_2(w)$ of (4.6), related to the boundary conditions $\overline{\psi}_1(+\infty) = 0$, $\overline{\psi}_2(-\infty) = 0$, which are expressed by

$$\overline{\psi}_1(w) = \sum_{n=0}^{\infty} \overline{f}(w+n) \qquad \overline{\psi}_2(w) = -\sum_{n=1}^{\infty} \overline{f}(w-n)\,. \tag{4.7}$$

Using Borel re-summation one can prove that $\overline{\psi}_1$, $\overline{\psi}_2$ are analytic on sectors [20–22], and have the same asymptotic expansion $\overline{\psi}(w) = \sum_k \overline{\psi}_k\, w^{-k-1}$: letting $\overline{\psi}_B(t) = \sum_k (\overline{\psi}_k/k!)t^k$ be the Borel transform of the formal series $\overline{\psi}(w)$, then the re-summed function can be defined by

$$\overline{\psi}(w) = \int_0^{e^{i\theta}\infty} e^{-tw} \overline{\psi}_B(t)\, dt \tag{4.8}$$

and analytic continuation is obtained by rotating the integration axis $\rho e^{i\theta}$ as far as the first singularity of $\overline{\psi}_B(t)$ is encountered. Indeed, if we take the Borel transform of the functional equation (4.6) one has

$$e^{-t}\overline{\psi}_B(t) - \overline{\psi}_B(t) = \overline{f}_B(t)\,. \tag{4.9}$$

If $f(z)$ is analytic in a disc of radius $r$ then $\overline{f}(w)$ is analytic in the exterior of a disc of radius $r^{-1}$ and $\overline{f}_B(t)$ is an entire function. As a consequence the only singularities of $\overline{\psi}_B(t)$ are poles on the imaginary axis at $t = 2\pi i k$ with $k \in \mathbb{Z} \setminus \{0\}$:

$$\overline{\psi}_B(t) = \frac{\overline{f}_B(t)}{e^{-t} - 1} = \sum_{k \in \mathbb{Z}\setminus\{0\}} \frac{\overline{f}_B(i\,2\pi k)}{t - i\,2\pi k}\,. \tag{4.10}$$

Since $\overline{f}(w)$ is analytic over $|w| > 1/r$, using (4.7) one immediately checks that $\overline{\psi}_1(w)$ and $\overline{\psi}_2(w)$ are analytic in two domains $D_1$, $D_2$ whose complements are obtained by translating the disc $|w| \leqslant r^{-1}$ to the left and to the right, respectively (see figures 7(*a*) and (*b*)). The image of $D_1$ in the $z$-plane is the union of a half-disc of radius $r$ in the $\mathrm{Re}\, z > 0$ half-plane and two half-discs of radius $r/2$ on the opposite side, and similarly for $D_2$ (see figures 7(*c*) and (*d*)).

We choose the example where $f(z)$ has a simple pole $f(z) = z^2(1 - az)^{-1}$ so that $\overline{f}(w) = [w(w-a)]^{-1}$ and $\overline{f}_B(t) = (e^{at} - 1)/a$. We demand that $a \in \mathbb{R}_+ \setminus \mathbb{Z}$, since if $a$ is

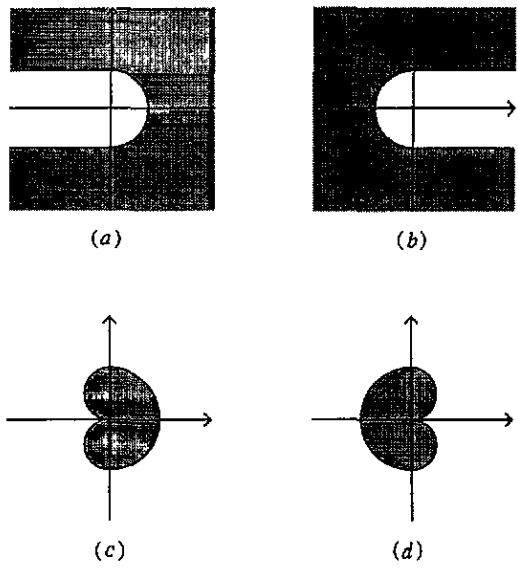


**Figure 7.** Sketch of the analyticity domain of $\psi_1$ in the ($a$) $w$- and ($c$) $z$-planes and the same for $\psi_2$ (($b$) and ($d$)).

an integer then the zeros of $e^{at} - 1$ exactly cancel the poles of the denominator of $\overline{\psi}_B(t)$. The domains $D_1$, $D_2$ are the complements of the sequences of points $w = -n$, $w = a - n$ for $n \geqslant 0$ and $w = n$, $w = a + n$ for $n \geqslant 1$ respectively. Integrating (4.8) along a line $t = \rho e^{i\theta}$ the analyticity domain of $\overline{\psi}(w)$ is determined by the growth of $|\overline{f}_B(t)|$; the non-analyticity domains $]-\infty, a]$ and $[0, +\infty[$ are not minimal but contain the previous ones, and their images in the $z$-plane are $]-\infty, 0] \cup [a^{-1}, +\infty]$ and $[0, +\infty[$, respectively.

In figure 8 we quote the poles of the [100/100] PA to $\overline{\psi}_B(t)$ computed with different accuracies. At low accuracy the presence of the noise circle is evident and there is no resemblance with the true analyticity structure. At very high accuracy a large number of poles on the imaginary axis is obtained together with their residues. Other poles lying on a large half-circle are stable against further increase of the accuracy and are due to the truncation of the series. Indeed the radius of the circle increases linearly with the order of the PA and these poles as $N \to \infty$ cluster at infinity to reproduce the essential singularity of the exponential function.

The behaviour of the PA for the function $\psi(z)$ is also quite interesting; indeed, in this case there are two functions $\psi_1$ and $\psi_2$ defined in the domains $D_1$ and $D_2$ with the same asymptotic expansion. The presence of the singularity at $z = 0$ makes the radius of the noise disc equal to zero as well. Indeed, at low accuracy there is a cluster of poles at 0 which disappear when the accuracy is sufficiently high (see figure 9($a$)). The poles of $\psi(z)$ in the plane $z$, computed with high precision (see figure 9($b$)), are distributed on a circle, whose radius appears to be $r = 1/(a + 1)$ to a good accuracy, and the values of the function in the inner and outer parts of the circle agree with $\psi_1$ and $\psi_2$ which can be obtained by numerically evaluating the integral (4.8). This structure can be understood by analysing the poles in the variable $w = 1/z$: the sequence of poles are distributed on two perpendicular axes, namely the real positive axis (where both determinations $\psi_1$ and $\psi_2$ have simple poles), and a line parallel to the imaginary axis, which corresponds to the cut placed by the PA: on the right-hand part of the plane $w$ (i.e. inside the circle in the $z$-plane), the PA re-sum the formal series to $\psi_1$, and on the left-hand part (i.e. outside the circle in the

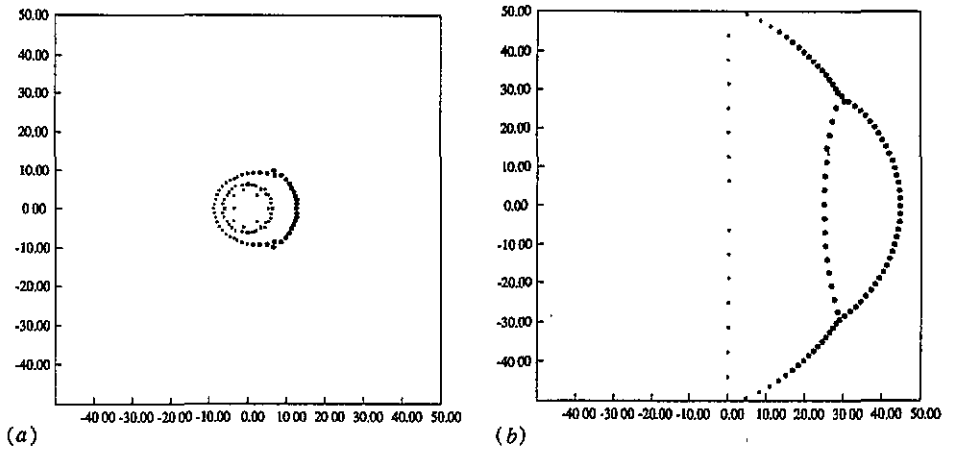


**Figure 8.** Poles of the [100/100] PA of $\Psi_B(t)$ solution of the homologic equation of a map tangent to the identity computed with low accuracy (*a*) $d = 16$ and high accuracy (*b*) $d = 200$.

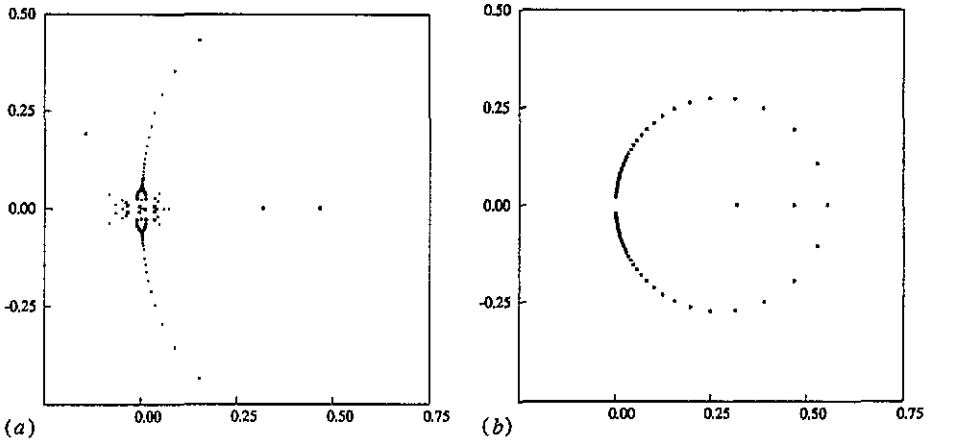


**Figure 9.** Poles of the [100/100] PA of $\Psi(z)$ for the homologic equation of a map tangent to the identity computed with low accuracy (*a*) $d = 16$ and high accuracy (*b*) $d = 200$.

$z$-plane), to $\psi_2$. The abscissa of the cut is the average of the first pole of $\psi_2$ (i.e. $w = 1$) and the last pole of $\psi_1$ (i.e. $w = a$). An exponential relation between the values of the residues and the distance of the position of the poles from the origin (in the $z$-plane) can be found and a complete characterization of the cut in the neighbourhood of the origin can be given; we refer to [35] for a complete analysis.

## 5. Conclusions

From the present analysis it emerges that the PA are adequate to describe the singularity pattern of the conjugation functions of holomorphic maps in the linearizable case, be it hyperbolic or parabolic, and even for a map tangent to the identity, provided that a sufficient accuracy is used. It must be pointed out that when a low number of digits is used the noise

disc obscures completely the true singularity structure. Singularity patterns symmetric with respect to the origin are better reproduced than asymmetric ones, regular patterns better than fractal patterns. When the singularities are on a circle, in order to distinguish the case of a probable natural boundary from a porous one, one has to use high-accuracy evaluations and careful inspection of the residues; otherwise a natural boundary will, in general, appear because the holes are filled by the noise poles.

## Acknowledgments

We would like to thank Dr Xie for the implementation of efficient algorithms to compute the PA, their poles and residues, using the very reliable MPA library of Brent. We are also indebted to Dr A Bazzani for very constructive discussions and Professor Servizi for advice on numerical computations.

## References

[1] Moser J 1973 *Stable and Random Motion in Dynamical Systems* (Princeton, NJ: Princeton University Press)
[2] Bazzani A and Turchetti G 1992 Singularities of normal formal forms and topology of orbits in area preserving maps *J. Phys. A: Math. Gen.* **25** 427
[3] Servizi G and Turchetti G 1990 Normal forms singularities in area preserving maps and analytic continuation by Padé approximants *Phys. Lett.* **151** 485
[4] Bessis D 1973 *Padé approximants* (London: Graves Morris)
[5] Turchetti G 1978 Variational matrix Padé approximants in two-body scattering *Fortschritte der Physik* **26** 1
[6] Mery P and Turchetti G 1975 Relativistic Green's function approximation to the low energy nucleon–nucleon interaction *Phys. Rev.* D **11** 2000
[7] Basdevant J L 1973 The Padé approximants and its physical applications *Fortschritte der Physik* **20** 283
[8] Berretti A and Chierchia L 1990 On the complex analytic structure of the golden invariant curve for the standard map *Nonlinearity* **3** 39
[9] Falcolini C and de La Llave R 1992 Numerical calculation of domains of analyticity for perturbation theories in presence of small divisors *J. Stat. Phys.* **67** 645
[10] Baker J and Graves Morris P 1981 Padé approximants *Encyclopedia of Mathematics* vol 13, 14 (New York: Addison-Wesley)
[11] Brolin H 1965 Invariant sets and iteration of rational functions *Arkiv für Matematik* **6** 103
[12] Siegel C L 1942 Iteration of analytic functions *Ann. Math.* **43** 607–12
[13] Gilewicz J and Truong-Van B and Froissart M 1988 Doublets in the Padé approximation and noise *Constructive Theory of Functions* (Sophia)
[14] Froissart M 1969 Application de Padé à la Physique des particules élémentaires CNRS, RP, Programme no 25, vol *9* 1–13
[15] Brent R P 1978 MPA: multiple precision floating point arithmetic *CERN Library Technical Report* 54
[16] Gammel J L and Nuttal J 1973 Convergence of Padé approximants to quasianalytic functions beyond natural boundaries *J. Math. Anal. Appl.* **43** 694
[17] Gammel J L 1974 Continuation of functions beyond natural boundaries *Rocky Mountain J. Math.* **4** 203
[18] Xie R 1993 Padé approximants applied to the singularity structure for conjugation problems *Chaos: Theory and Practice* ed Bountis (Berlin: Springer)
[19] Blanchard P 1984 Complex analytic dynamics on the Riemann sphere *Bull. Am. Math. Soc.* **11** 85–141
[20] Malgrange B 1982 Travaux d'Ecalle et de Martinet-Ramis sur les systèms dynamiques/Astérisque **92–93** 59–72
[21] Ecalle J 1982 *Les Fonctions Résurgentes et Leurs Applications* (Orsay: Publications Math. d'Orsay)
[22] Kimura T 1971 On the iteration of analytic functions *Funk. Equacioj* **14–3** 197–238
[23] Elizarov P M 1985 Orbital analytical nonequivalence of saddle resonance vector fields in $(\mathbb{C}^2, 0)$ *Math. USSR Sbornik* **51** 533–47
[24] Pomerenke C 1973 Padé approximants and convergence in capacity *J. Math. Anal. Appl.* **41** 775
[25] Zinn Justin J 1971 Padé approximants *Phys. Rep.* **3** 55

[26] Bharucha-Reid A T and Sambandham M 1986 *Random Polynomials* (New York: Academic)
[27] Szego H 1939 *Orthogonal Polynomials* (New York: American Mathematical Society)
[28] Brjuno A D 1971 Analytic form of differential equations *Trans. Mosc. Math. Soc.* **25** 131–288
[29] Billi L *et al* 1993 Natural boundaries for Hamiltonian maps and the genesis of the Siegel disc *Preprint* University of Bologna
[30] Percival I C and Greene J M 1981 Hamiltonian maps in the complex plane *Physica* **3D** 530
[31] Percival I C 1982 Chaotic boundary of a Hamiltonial map *Physica* **6D** 67
[32] Voronin S M 1981 Analytic classification of germs of conformal mappings $(\mathbb{C}, 0) \to (\mathbb{C}, 0)$ with identity linear part *Funct. Analy. Appl.* **15** 1–12
[33] Camacho C 1978 On the local structure of conformal mappings and holomorphic vector fields in $\mathbb{C}^2$ *Astérisque* **59–60** 83–95
[34] Martinet J and Ramis J P 1983 Classification analytique des équations différentielles nonlinéaires résonnantes du premier ordre *Ann. Scient. Éc. Norm. Sup.* **16** 571–621
[35] Todesco E 1994 Geometria delle risonanze in sistemi dinamici discreti Hamiltoniani e olomorfi *PhD thesis* University of Bologna